Available online at www.sciencedirect.com
ScienceDirect
Journal of Solid State Chemistry 180 (2007) 792–798
JOURNAL OF SOLID STATE CHEMISTRY
www.elsevier.com/locate/jssc

Rapid communication

Synthesis, characterization, and electrochemical properties of ordered mesoporous carbons containing nickel oxide nanoparticles using sucrose and nickel acetate in a silica template

Yulin Cao, Jieming Cao*, Mingbo Zheng, Jinsong Liu, Guangbin Ji

Nanomaterials Research Institute, College of Material Science and Technology, Nanjing University of Aeronautics and Astronautics, Nanjing 210016, PR China

Received 14 September 2006; received in revised form 26 October 2006; accepted 30 October 2006
Available online 3 November 2006

Abstract

New ordered mesoporous carbons containing nickel oxide nanoparticles have been successfully synthesized by carbonization of sucrose in the presence of nickel acetate inside SBA-15 mesoporous silica template. The obtained samples were characterized by X-ray diffraction (XRD), nitrogen adsorption–desorption, and transmission electron microscopy (TEM). The NiO nanoparticles were embedded inside the mesoporous carbon framework due to the simultaneous pyrolysis of nickel acetate during carbonization. The electrochemical testing of the as-made nanocomposites showed a large specific capacitance of 230 F g^{-1} using 2 M KOH as the electrolyte at room temperature. This is attributed to the nanometer-sized NiO formed inside mesoporous carbons and the high surface area of the mesopores in which the NiO nanoparticles are formed. Furthermore, the synthetic process is proposed as a simple and general method for the preparation of new functionalized mesoporous carbon materials, for various applications in catalysis, sensor or advanced electrode material.

Keywords: Ordered mesoporous carbon; Nickel oxide nanoparticle; Nanocomposite; Electrochemical property

1. Introduction

The synthesis of ordered mesoporous carbons (OMCs) using mesoporous silica as hard templates has received much attention in the recent years. OMCs can be available with various structures such as cubic *Ia3d*, *Fm3m*, *Im3m*, and 2-dimensionally (2D) hexagonal *P6mm*. The successful synthesis of carbon with an ordered pore structure was firstly achieved using MCM-48 as templates to create a carbon material (CMK-1) [1]. The pore diameter and pore-wall thickness of mesoporous carbons could be easily tailored through controlling the structure of the silica template and other details of the synthesis conditions [2]. Various organic compounds such as sucrose [1–3], furfuryl alcohol [4], phenol resin [5], mesophase pitch [6], polydivinylbenzene [7], acrylonitrile [8], pyrrole [9], and polystyrene-based polymer [10], are suitable as the carbon precursors. The carbon precursors are impregnated into mesoporous silica with a special structure to give a desired composition, followed by carbonization of the precursor in the pore system to result in a carbon–silica composite. Finally, the structural order of the carbon framework can be retained after the silica template is removed with NaOH or HF solution. The resulting OMC material has an extremely high surface area, a large pore volume, excellent mechanical stability, good thermal stability and electrical conductivity, which make the resulting OMCs promising candidates for catalyst supports, absorbents, hydrogen storage media, and advanced electrodes [4,11].

Sucrose is most widely used as a carbon source for the preparation of OMC materials. Sucrose could be completely incorporated into the channels of mesoporous silica templates by a controllable two-step impregnation process.

*Corresponding author. Fax: +86 25 8489 5289.
E-mail address: jmcao@nuaa.edu.cn (J. Cao).

0022-4596/$ - see front matter © 2006 Elsevier Inc. All rights reserved.
doi:10.1016/j.jssc.2006.10.024

After carbonization of the precursors at 1173 K and dissolution of the templates by using HF solution, the obtained OMCs maintain the macroscopic morphology and ordered mesostructures of the templates. The impregnation can be carried out by the addition of metal acetates into sucrose. The pyrolysis of metal acetate during the carbonization can lead to generate metal-oxide nanoparticles. The simultaneous pyrolysis and carbonization is particularly attractive because the metal oxide may be incorporated in the final OMC product, thus affording the possibility to prepare functionalized OMC materials containing such metal-oxide nanoparticles. OMC materials containing such nanoparticles may find suitable applications for the development of heterogeneous catalysts, adsorbents and advanced electrode materials [12–14].

Recently, OMCs have drawn great interest due to the application as electrochemical double-layer capacitor. Furthermore, nickel oxide is easily available and possesses a high specific capacitance that is comparable with carbon materials [15]. Encapsulation of electroactive substances can result in Faradic pseudocapacitance. Therefore, NiO-OMC composites are expected to provide a chance to improve the capacitor performance. However, the reports on NiO-OMC composites have not been frequent in the literature. Li et al. synthesized ordered mesoporous nickel oxide/carbon (NiO/C) nanocomposites by a procedure that combines nanocasting with thermolysis [16]. Nevertheless, the whole process was multi-step and time consuming because the impregnation procedure of carbon and nickel nitrate precursor was separated. Also, only structure characterization results were presented, while the study of the composite electrochemical properties was absent.

Here we report a new procedure for synthesizing a new OMC-nickel oxide nanocomposite using sucrose and nickel acetate precursors in a mesoporous silica. SBA-15 silica was selected as a template for the OMC materials. The carbon precursors are converted to a rigid, 3-D carbon framework in SBA-15 mesoporous silica templates, following a high-temperature carbonization process. The nickel oxide nanoparticles were formed due to the simultaneous pyrolysis of the metal acetate during carbonization inside the mesoporous pores of SBA-15. The synthesis results showed that metal-oxide nanoparticles were embedded inside the mesoporous carbon particles. The OMC products containing the nanoparticles were attractive due to the ordered hexagonal structure and two different composite components, suggesting strong potential for application in electrochemical capacitor and catalysis. The obtained materials were characterized by means of X-ray diffraction (XRD), nitrogen adsorption–desorption isotherm measurements, and transmission electron microscopy (TEM). Furthermore, the electrochemical properties of the NiO-containing mesoporous carbons were for the first time measured, showing a large specific capacitance of 230 $F\,g^{-1}$ using 2 M KOH as the electrolyte at room temperature.

2. Experimental

2.1. Synthesis

The SBA-15 silica was synthesized following the procedure reported by Zhao et al. [17]. In a typical synthetic process, 4.0 g of the structure-directing triblock copolymer poly(ethylene oxide)–poly(propylene oxide)–poly(ethylene oxide), $EO_{20}PO_{70}EO_{20}$ (Pluronic 123, BASF) was dissolved in 30 g of deionized water and 120 g of 2 M HCl solution with stirring at 313 K. Then 8.50 g of tetraethyl orthosilicate (TEOS, AR) was added and the resulting mixture was stirred at 313 K for 20 h. The milky mixture was transferred into an autoclave and aged for 2 days at 373 K. The solid was separated by filtration, washed with deionized water, dried at room temperature, and calcined in air at 773 K for 6 h to obtain SBA-15.

The overall synthesis scheme for the NiO-containing mesoporous carbon can be illustrated in Fig. 1. The NiO-containing carbon is designated as NiOCMK. This novel procedure is based on the pyrolysis of sucrose and nickel acetate as precursors in mesoporous silica SBA-15 template. The substrate infiltrated with nickel acetate and carbon precursors was then subjected to carbonization at 1173 K under nitrogen atmosphere, followed by removal of the silica template with HF solution, washing, and drying to obtain the final NiOCMK materials. Unlike the more conventional replication procedure for the synthesis of

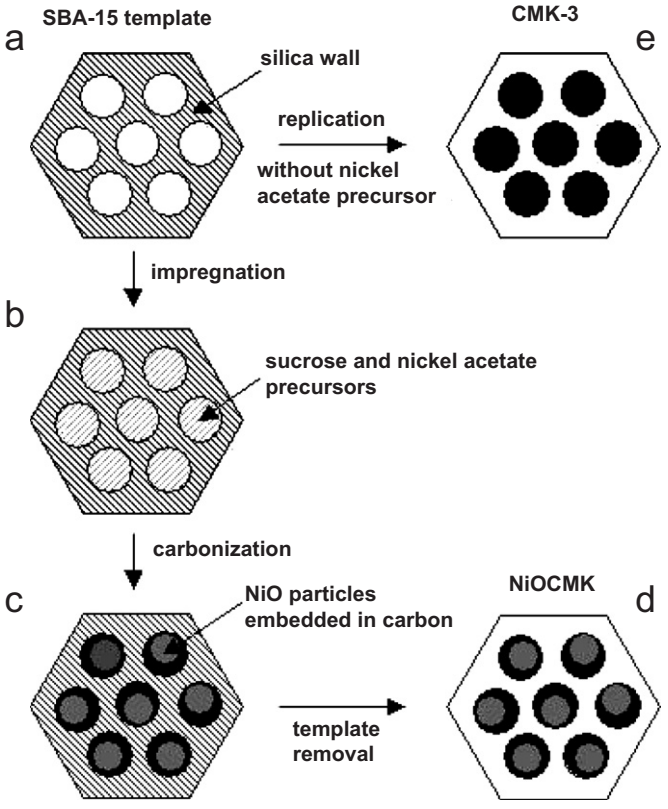

Fig. 1. Schematic drawings of synthesis routes for (a)→(d) NiOCMK and (a)→(e) CMK-3.

rod-like mesoporous carbon CMK-3, which may be achieved in the absence of an NiO precursor, the synthetic route reported here results in uniform formation of NiO nanoparticles in the pore network of the rod-like carbons. In a typical process, 1 g of calcined SBA-15 was added to a solution obtained by dissolving 1.00 g of sucrose, 0.25 g of nickel acetate, and 0.02 mL of 10 M H_2SO_4 in 5 g of H_2O. The mixture was placed in a drying oven for 6 h at 373 K, and subsequently the oven temperature was increased to 433 K and maintained there for 6 h. The silica sample was treated again at 373 and 433 K using the same drying oven after the addition of 0.64 g of sucrose, 0.16 g of nickel acetate, 0.01 mL of 10 M H_2SO_4, and 5 g of H_2O. The carbonization was completed by pyrolysis with heating to typically 1173 K under nitrogen atmosphere. The carbon–silica composite obtained after pyrolysis was washed with hydrofluoric acid at room temperature, to remove the silica template. The template-free carbon product thus obtained was filtered, washed with ethanol, and dried at 393 K. The loading of NiO in final product was circa 10 wt% calculated by thermal analysis. The carbon was almost completely removed below 1073 K in air and the remaining weigh was assumed to be NiO.

2.2. Characterization

Powder XRD patterns were recorded with a Bruker AXS D8 Advance diffractometer operating with Cu Ka radiation at 1.5 kW. For measurement with $2\theta < 10^\circ$, the step width and acquisition time were 0.01θ and 1.0 s, respectively; 0.02θ and 0.5 s were employed for wider angles.

Nitrogen adsorption–desorption isotherms were obtained with a Micromeritics ASAP2010 instrument at 77 K. Samples were outgassed for 10 h under vacuum at 573 K before measurement. The specific surface area was calculated using the Brunauer–Emmet–Teller (BET) equation, using data in the P/P_0 region between 0.05 and 0.15 [18]. The Barret–Joyner–Halenda (BJH) method was applied to analyze the mesopore size distributions using the adsorption branch [19]. Total pore volume was estimated from the amount of nitrogen adsorbed at a relative pressure of about 0.95.

For TEM, powder samples were dispersed in ethanol with sonication. Porous carbon grids were dipped into the suspension, and the dried grids were used. TEM images were obtained with a FEI Tecnai-20 instrument operating at 200 kV.

The obtained powders were used to fabricate the electrode of electrochemical capacitors according to the previous report [20]. The electrode was formed by mixing 80 wt% active material, 15 wt% acetylene black and 5 wt% PTFE as binder before rolling into a thin sheet of uniform thickness. Pellets cut out of the sheet were pressed with a hand oil press onto an Ni-foam current collector ($2 \times 2\,cm^2$). The electrode performance was measured in a beaker-type electrochemical cell equipped with the working electrode, a platinum counter electrode, and a standard calomel reference electrode. The performance of the as-prepared electrode was measured with a CHI660 electrochemical working station using 2 M KOH as the electrolyte at room temperature in air.

3. Results and discussion

3.1. X-ray diffraction (XRD)

Fig. 2 shows the low-angle XRD patterns of the calcined SBA-15 and corresponding NiOCMK nanocomposite. The SBA-15 sample shows three resolved peaks that can be basically indexed as (100), (110), and (200) reflections associated with the 2-D hexagonal *P6mm* symmetry, indicating the ordered arrangement of the nanopores in SBA-15. The (100) peak reflects a d spacing of 10.6 nm.

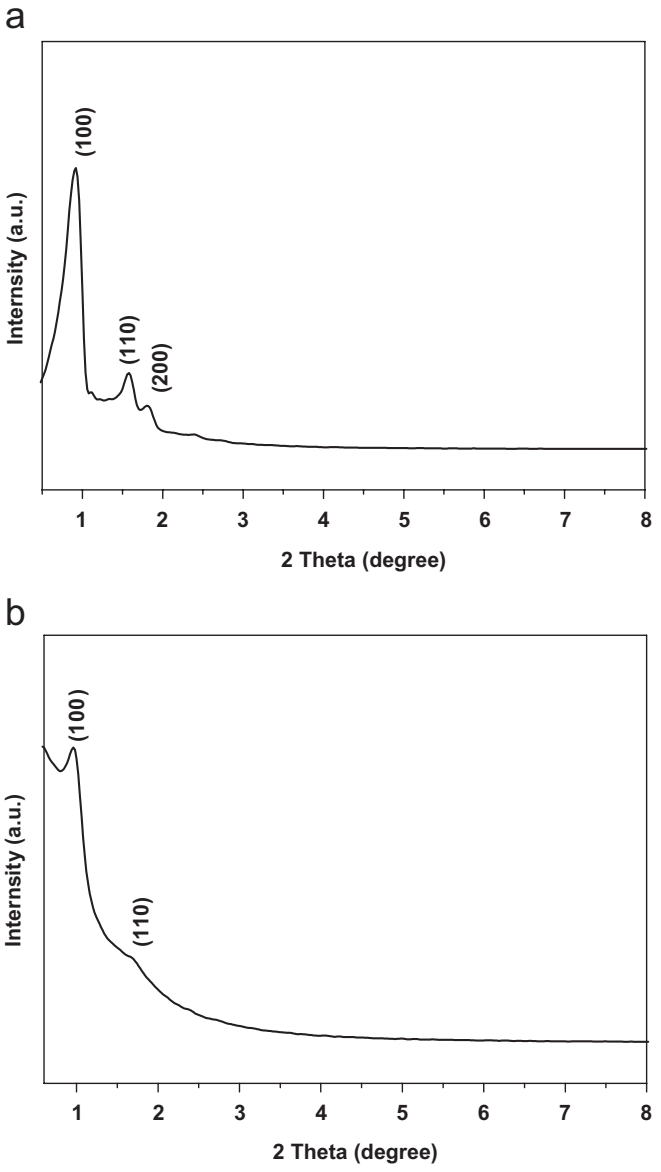

Fig. 2. The low-angle XRD patterns of (a) the SBA-15 silica template and (b) the corresponding NiOCMK materials.

No diffraction peak was observed in the region of higher angles (8–80°), which indicates the absence of large crystals in the sample, suggesting that SBA-15 sample is a pure phase.

It is notable that NiOCMK composite is not as ordered as SBA-15. The low-angle XRD patterns of the NiOCMK product show characteristic reflections of the *P6mm* hexagonal structure, although the higher-order reflections are not very profound or well-resolved. A unit-cell parameter of 10 nm was calculated from the position of (100) reflection, which is slightly smaller than that of the starting SBA-15 material ($a = 10.6$ nm).

Fig. 3 exhibits the wide-angle XRD patterns of the NiOCMK materials. The wide-angle diffraction patterns of NiOCMK show three broad Bragg diffraction peaks of nickel oxide phase, suggesting that this nickel oxide is readily crystallized within the confined nanospace. The microscopic structure of the nickel oxide is face-centered cubic (Powder Diffraction File Database (PDF-2) entry: 42-1049), corresponding to the crystalline structure known to exist for the bulk materials. The wide-angle XRD patterns of NiOCMK also show a broad diffraction peak near 2θ ca. 20–30°. In fact, the broad peak indicates that OMC includes very small amounts of stacked crystalline graphite phase, which is similar to the wide-angle XRD results of CMK-3 with an individual diffraction peak of graphite (002) at ~26° [21]. No indication of other impurity phase was observed in the XRD analysis. It is noteworthy that no Ni metal phase appeared in carbon framework during calcination despite the reducing nature of the carbon. Presently, the reason is not fully understood but the carbon framework may reduce the surface energy of NiO, which would passivate and stabilize the NiO nanoparticles. Previously, Huwe et al. [13] have also reported the synthesis of Fe_2O_3 nanoparticles within the mesopores of CMK-1 mesoporous carbons without reduction. The broadening of NiO peaks in the XRD pattern is due to the small particle size. The high-temperature carbonization of precursors in confined space can result in a rigid, 3-D carbon network with small NiO nanoparticles in carbon framework. This may explain the broadening peaks of wide-angle XRD patterns of NiOCMK composite.

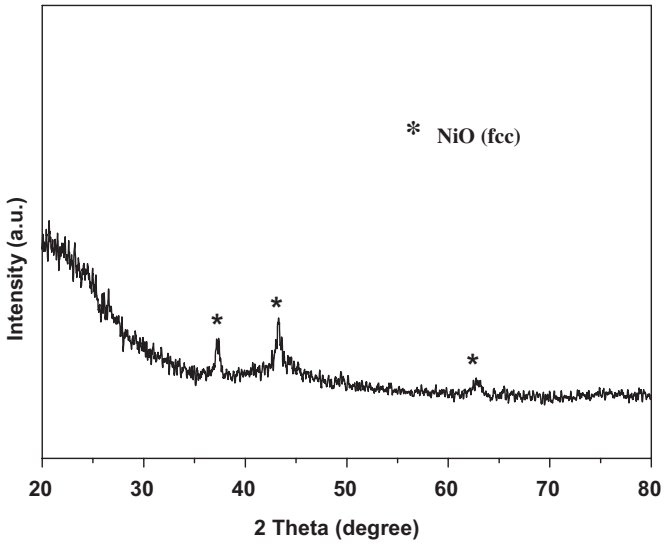

Fig. 3. The wide-angle XRD patterns of the NiOCMK materials.

3.2. Nitrogen adsorption–desorption isotherms

Fig. 4 shows adsorption–desorption isotherms of calcined SBA-15 and NiOCMK, and the pore size distribution (PSD) curves obtained from the adsorption branch. Both samples give typical type-IV isotherms with a sharp inflection at relative pressure $P/P_0 > 0.4$, characteristic of capillary condensation, which indicate the uniformity of the mesopore size distribution. PSD of SBA-15 is centered at 9.8 nm. The pore-wall thickness of SBA-15 is circa 0.8, which can be calculated from low-angle XRD data and

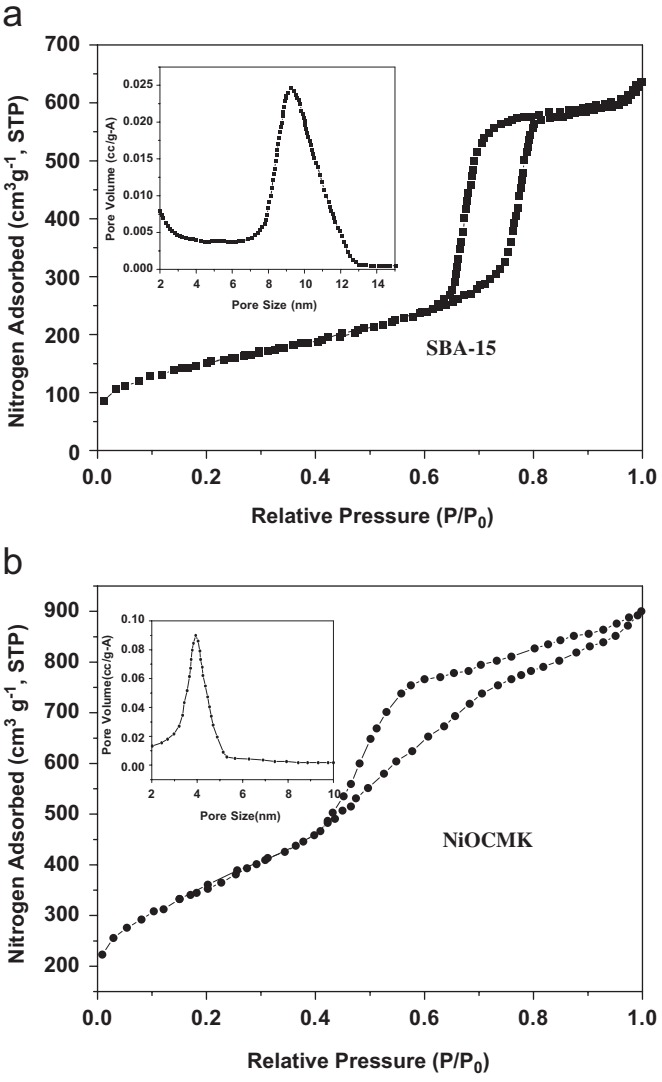

Fig. 4. Nitrogen adsorption–desorption isotherms of mesoporous silica SBA-15 and NiOCMK materials. The pore diameters, calculated by BJH method from the adsorption branch, are shown in the inset.

nitrogen adsorption–desorption analysis. The BET specific surface area and pore volume of SBA-15 are $580\,m^2\,g^{-1}$ and $1.02\,cm^3\,g^{-1}$, respectively. This is similar to previous reports about SBA-15 [17].

For the NiOCMK material, the PSD is mainly located at 3–5 nm, and the average pore size is centered at 3.9 nm by BJH algorithm calculated from the adsorption branch. Some typical textural parameters of NiOCMK are BET surface area of $1262\,m^2\,g^{-1}$ and pore volume of $1.38\,cm^3\,g^{-1}$, the latter being primarily related to the volume of the ordered pores, with minor contribution from secondary micropores. The pore-wall thickness of NiOCMK is calculated from adsorption and XRD data to be circa 6.1 nm. The pore-wall thickness is thus smaller than the pore diameter of SBA-15. This may be attributed from the structure shrinkage of precursors during calcination, which is similar to the structure change of highly OMC CMK-3 from SBA-15 template [3].

SBA-15 silica is a mesoporous material with a 2D hexagonal structure, in which 1D mesoporous channels are randomly interconnected through complementary pores. The uniform, regular ordered mesopores inside SBA-15 provide a confined space for nanoscale reaction. The mixed aqueous solution of sucrose and nickel acetate can easily impregnate into the mesopores of SBA-15. The white impregnated sample changes to dark brown upon heating to 373 K in the SBA-15 template containing nickel acetate. The color change is due to the formation of conjugated double bonds in the molecules [22]. After calcination, the precursors inside the mesopores of SBA-15 turn into a hexagonal array of carbon nanorods, which is interconnected with randomly distributed smaller carbon nanorods, with nickel oxide particles generated inside the carbon framework.

The NiOCMK materials retain the high specific surface area and large pore volume, which are essential for the use of NiOCMK as electrode materials of electrochemical capacitor. Large specific surface areas can store more energy, and the regular mesopore array can facilitate the diffusion of the electrolytes to the active surface of the nanocomposites.

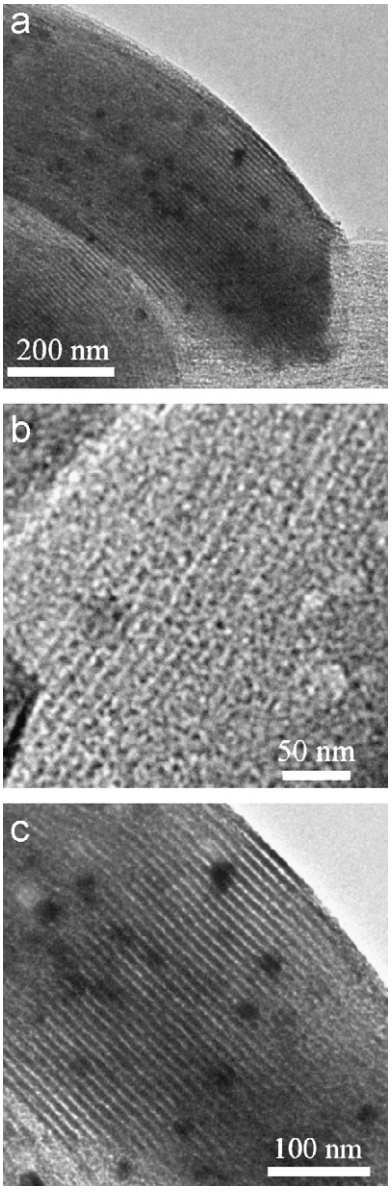

Fig. 5. (a) Typical TEM image of the as-made NiOCMK materials recorded perpendicular to the mesoporous orientation. (b,c) High-magnification TEM images of the NiOCMK materials.

3.3. Transmission electron microscope (TEM)

Fig. 5 shows the typical TEM images for the NiOCMK sample viewed perpendicular to the direction of the ordered pore arrangement. The stripe patterns in the background of the images can be assigned to the lattice fringes of the *P6mm* mesostructure of the carbon. As the TEM images show, the carbon nanorods in NiOCMK are 8.8 nm in diameter. There are smaller interconnecting carbon rods in the NiOCMK materials. The main mesoporous channels in SBA-15 are interconnected through micropores inside the walls of the main channels. In the case of SBA-15 silica, carbon infiltration leads to the formation of carbon rods that are bonded to each other. Therefore, the hexagonal structural order is retained in the NiOCMK materials. The pore diameter of SBA-15 (9.8 nm) is larger by approximately 1 nm than the diameter of carbon nanorods. The center-to-center distances of adjacent channels are about 10 nm, which is in reasonable agreement with the XRD analysis.

The dark spots in diameter are the images of the NiO nanoparticles. It is very interesting to find that there are two kinds of particle size distributions of NiO nanoparticles in the NiOCMK materials. The particle sizes of NiO are deduced from TEM images. The main particle diameters are 8 and 26 nm, respectively. For 8 nm NiO particles, these nanoparticles are slightly smaller than the diameters of carbon nanorods. It has been confirmed that most of the smaller NiO nanoparticles (about 90%) are embedded inside the OMC nanorods, from TEM images

taken with sample tilting at various angles. On the other hand, the sizes of other NiO nanoparticles (26 nm) are much larger than the diameters of carbon nanorods or even the lattice parameter (10 nm) of the mesoporous carbons. Such NiO particles (about 10%) seem to grow to these sizes through the interconnecting mesopores. Initially, the nickel acetate precursors can form small NiO particles inside the mesopores at lower temperature. The particle diameters at the corresponding NiO loading increase to larger sizes, as the synthesis temperature is increased to 1173 K. This may explain the two different particle size distributions of NiO species. Thus OMC is used as a host material to support these well-dispersed NiO particles and retain the mesoporous system.

3.4. Electrochemical properties

Fig. 6 shows the cyclic voltammograms (CVs) of the NiOCMK electrode at a sweep rate of $20\,mV\,s^{-1}$ in the voltage range from -0.2 to 0.35 V. The CVs exhibit two current peaks that relate to the Faradaic reaction at the surface of NiO. In the voltage range of -0.2 to 0.05 V, the CVs show a partial rectangular shape, suggesting the electrical double-layer reaction of mesoporous carbon materials.

The NiOCMK electrode has a large specific capacitance of $230\,F\,g^{-1}$ at a sweep rate of $20\,mV\,s^{-1}$, which is calculated according to the formula reported in the literature [23]. Such correct performance of this electrochemical capacitor is confirmed by the galvanostatic charge/discharge characteristics at a current density of $1200\,mA\,g^{-1}$ presented in Fig. 7. The capacitance value of CMK-3 was $170\,F\,g^{-1}$ at the sweep rate of $20\,mV\,s^{-1}$ using KOH as the electrolyte at room temperature according to the previous literature [24]. So the NiOCMK electrode reveals the capacitance improvement contributed from NiO nanoparticles. Although the NiO nanoparticles are

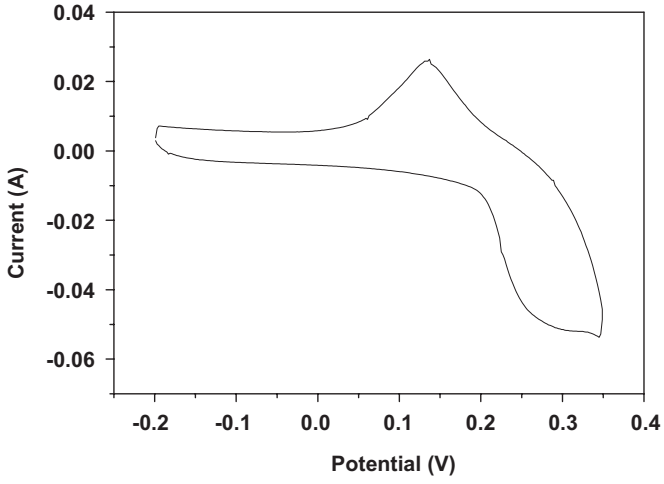

Fig. 6. Cyclic voltammograms (CVs) of the NiOCMK materials at a sweep rate of $20\,mV\,s^{-1}$ using 2 M KOH as the electrolyte at room temperature.

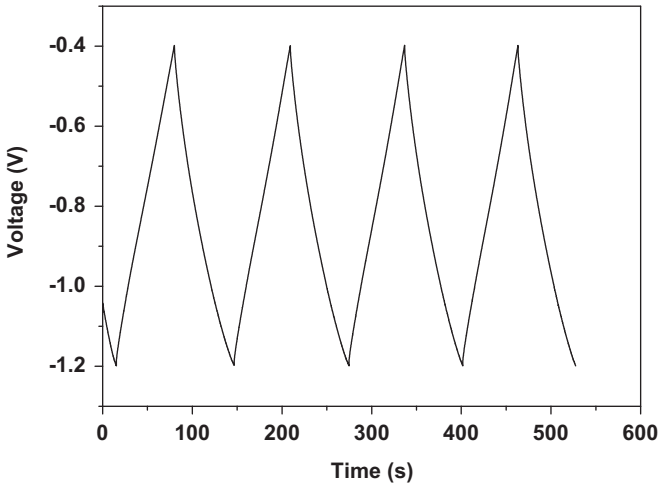

Fig. 7. Galvanostatic charge/discharge of the electrochemical capacitor built from the NiOCMK nanocomposite; current density is $1200\,mA\,g^{-1}$.

studded in the carbon lattices, these NiO particles could also be accessible to the electrolyte in the liquid phase. Besides the electrical double-layer reaction of mesoporous carbon materials in electrochemical test, the Faradaic reaction at the surface of NiO can still contribute to the total electrochemical properties. The two different composite components are profitable for the performance of these templated carbons, but also the sizes and the arrangement of their pores may play an important role. Generally, the better accessibly the ions can favor into the electrochemically active surface, the higher the value of capacitance is. Although, taking into account that the surface areas determined by nitrogen adsorption and the electrochemically active surface areas are different, the main parameter controlling the electrochemical performance in these materials is the total surface area. Other factors might also be profitable for the electrochemical properties, for example (a) the different pore arrangement which favors the diffusion of the solvated ions; (b) the presence of a more marked secondary microporosity for NiOCMK.

4. Conclusion

The carbon synthesis using sucrose in a mesoporous silica template is a versatile route for obtaining OMCs with various structures. We have demonstrated that the template-directed method can be extended to the facile synthesis of mesoporous carbons containing transition metal-oxide nanoparticles, through the use of SBA-15 silica templates containing nickel acetate. Initially, the metal acetate and sucrose precursors can impregnate into the mesopores of the SBA-15 template, followed by full carbonization through heating under a nitrogen atmosphere at ambient pressure. The metal species are spontaneously decomposed during the carbonization process, forming metal-oxide nanoparticles. The carbon synthesis can be controlled for faithful replication of template structures, where metal-oxide nanoparticles are

embedded within the carbon structure. The preliminary results of electrochemical properties are also described, which demonstrates a large specific capacitance of $230\,F\,g^{-1}$ owing to nanometer-sized NiO formed inside mesoporous carbons, the high surface area as well as mesopores formed among nanoparticles for electrolyte accessible. Such OMCs containing metal-oxide nanoparticles may find applications in catalysis and electrochemistry. Moreover, this synthetic method may extend to prepare new OMC nanocomposites containing other nanoparticles for different applications in chemical sensors, high-density electronic devices and lithium-ion batteries.

Acknowledgments

We acknowledge the financial supports of National Natural Science Foundation of China (Grant no. 50502020) and Natural Science Foundation of Jiangsu Province (Grant no. BK2006195).

Reference

[1] R. Ryoo, S.H. Joo, S. Jun, J. Phys. Chem. B 103 (1999) 7435.
[2] J.S. Lee, S.H. Joo, R. Ryoo, J. Am. Chem. Soc. 124 (2002) 1156.
[3] S. Jun, S.H. Joo, R. Ryoo, M. Kruk, M. Jaroniec, Z. Liu, T. Ohsuna, O. Terasaki, J. Am. Chem. Soc. 122 (2000) 10712.
[4] S.H. Joo, S.J. Choi, I. Oh, J. Kwak, Z. Liu, O. Terasaki, R. Ryoo, Nature 42 (2001) 169.
[5] J. Lee, S. Yoon, T. Hyeon, S.M. Oh, K.B. Kim, Chem. Commun. (1999) 2177.
[6] Z. Li, M. Jaroniec, J. Am. Chem. Soc. 123 (2001) 9208.
[7] S.B. Yoon, J.Y. Kim, J.S. Yu, Chem. Commun. (2002) 1536.
[8] A.H. Lu, A. Kiefer, W. Schmidt, F. Schüth, Chem. Mater. 16 (2004) 100.
[9] C.M. Yang, C. Weidenthaler, B. Spliethoff, M. Mamatha, F. Schüth, Chem. Mater. 17 (2005) 355.
[10] C.O. Ania, T.J. Bandosz, Micropor. Mesopor. Mater. 89 (2006) 315.
[11] R. Ryoo, S.H. Joo, M. Kruk, M. Jaroniec, Adv. Mater. 13 (2001) 677.
[12] J. Lee, S. Jina, Y. Hwang, J.G. Park, H.M. Park, T. Hyeon, Carbon 43 (2005) 2536.
[13] C. Minchev, H. Huwe, T. Tsoncheva, D. Paneva, M. Dimitrov, I. Mitov, M. Fröba, Micropor. Mesopor. Mater. 81 (2005) 333.
[14] S. Zhu, H. Zhou, M. Hibino, I. Honma, M. Ichihara, Adv. Funct. Mater. 15 (2005) 381.
[15] K.W. Nam, W.S. Yoon, K.B. Kim, Electrochim. Acta 47 (2002) 3201.
[16] H. Li, S. Zhu, H. Xi, R. Wang, Micropor. Mesopor. Mater. 89 (2006) 196.
[17] D. Zhao, J. Feng, Q. Huo, N. Melosh, G.H. Fredrickson, B.F. Chmelka, G.D. Stucky, Science 279 (1998) 548.
[18] S. Brunauer, P.H. Emmett, E. Teller, J. Am. Chem. Soc. 60 (1938) 309.
[19] E.P. Barrett, L.G. Joyner, P.P. Halenda, J. Am. Chem. Soc. 73 (1951) 373.
[20] F.B. Zhang, Y.K. Zhou, H.L. Li, Mater. Chem. Phys. 83 (2004) 260.
[21] H. Zhou, S. Zhu, M. Hibono, I. Honma, M. Ichihara, Adv. Mater. 15 (2003) 2107.
[22] M. Choura, N.M. Belgacem, A. Gandini, Macromolecules 29 (1996) 3839.
[23] V. Srinivasan, J.W. Weidner, J. Electrochem. Soc. 147 (2000) 880.
[24] W. Xing, S.Z. Qiao, R.G. Ding, F. Li, G.Q. Lu, Z.F. Yan, H.M. Cheng, Carbon 44 (2006) 216.